Journal of Alloys and Compounds 506 (2010) 73–76

Contents lists available at ScienceDirect

Journal of Alloys and Compounds

journal homepage: www.elsevier.com/locate/jallcom

Studies on ferromagnetic shape memory Ni–Mn–Ga alloys with Fe and rare-earths additives

R.K. Singh [a,*], M. Manivel Raja [a], R.P. Mathur [a], M. Shamsuddin [b]

[a] Defence Metallurgical Research Laboratory, Hyderabad 500 058, India
[b] Department of Metallurgical Engineering, Institute of Technology, Banaras Hindu University, Varanasi 221 005, India

ARTICLE INFO

Article history:
Received 11 June 2010
Accepted 24 June 2010
Available online 24 July 2010

Keywords:
Ferromagnetic shape memory alloy
Martensite transformation
Magnetic properties

ABSTRACT

The effect of Fe and rare-earths (Tb&Dy) addition on the martensitic transformation, magnetic and mechanical properties of the $Ni_{50}Mn_{30}Ga_{20}$ (at%) ferromagnetic shape memory alloy was investigated. The results show that the rare-earths exhibit negligible solubility in the Ni–Mn–Ga–Fe matrix phase and formed grain boundary phase. The grain boundary precipitate enhances the compressive ductility of the alloys. The martensite transformation temperature was found to be increased by the addition of rare-earths, while, Fe increased the Curie temperature of the Ni–Mn–Ga alloy. However, with increase in Fe content, an additional $(Ni,Fe)_3(MnGa)$ precipitate is formed, leading to decrease in martensite transformation temperature and compressive ductility.

1. Introduction

Ferromagnetic shape memory (FMSM) alloys based on Ni–Mn–Ga have been widely investigated as promising actuator materials due to their large magnetic field induced strains (MFIS) and high response frequency [1,2]. The large MFIS is associated with the coupling between the crystal structure and the magnetism to enable rearrangement of martensite twin variants by an external magnetic field [3]. These martensite twin variants are formed as a result of thermoelastic martensite transformation, which involves transformation of ordered cubic $L2_1$ austenite phase to a low-symmetry non-modulated tetragonal or modulated (5M,7M) martensite phases depending on the alloy composition [4]. From application point of view, Ni–Mn–Ga alloys have some limitations in terms of temperature dependence of MFIS, low martensite transformation (T_M), Curie (T_C) temperatures and high brittleness in polycrystalline state. In this context, it has been found that Fe substitution for Mn/Ni in ternary Ni–Mn–Ga alloys improves thermal stability of MFIS, ductility and magnetic properties of the alloy [5–10]. However, the martensite transformation in general shifts to lower temperature along with increase in the hysteresis of transformation [8,11–13]. On the other hand, it is reported that minor addition of rare-earths in ternary Ni–Mn–Ga alloys can adjust the martensite transformation to higher temperatures [14–18]. Moreover, addition of rare-earth elements enhances the mechanical properties of Ni–Mn–Ga alloys by forming grain boundary precipitate. Nevertheless, the Curie temperature either remains unchanged or decreases with rare-earth additions [15,17]. Therefore, in the present study, we have carried out both Fe and rare-earth additions in a polycrystalline Ni–Mn–Ga alloy; with intend to beneficially modify its phase transformation temperature and magnetic properties. Alloying was carried out by substituting fixed amount of rare-earths (1 at% Dy and 0.5 at% Tb) for Ga atoms and variable amount of Fe for the Mn atoms in a reference $Ni_{50}Mn_{30}Ga_{20}$ (at%) alloy composition to study the effect of alloying on the structure and properties of the magnetic shape memory alloy.

2. Experimental details

Three polycrystalline alloys, with nominal composition $Ni_{50}Mn_{30}Ga_{20}$, $Ni_{50}Mn_{25}Fe_5Ga_{18.5}R_{1.5}$, and $Ni_{50}Mn_{20}Fe_{10}Ga_{18.5}R_{1.5}$ (numbers indicate at% and R stands for rare-earths 1 at% Dy and 0.5 at% Tb), designated hereafter as alloys NMG, FE5 and FE10, were prepared by arc melting of high purity elements under argon atmosphere. All the alloys were melted four times and turned in between melts to obtain homogeneity. The as-cast alloys were sealed in quartz tubes under high vacuum and annealed at 1273 K for 72 h and at 1073 K for 48 h, followed by water-quenching in order to obtain high ordering. The electron probe microanalysis (EPMA) technique was used to determine the chemical composition of the constituent phases and microstructure. The room temperature crystal structure was studied using Philips PW1320 diffractometer with Cu Kα radiation. The phase transformation temperatures were determined by differential scanning calorimeter (DSC) model Q100 (make TA instruments, USA) under a constant heating/cooling rates of 20 K/min. Vibrating sample magnetometer (EV9 model, ADE make, USA) was used for magnetic characterization. The compression tests were performed on a mechanical testing system (make BISS, India) at a crosshead displacement speed of 0.05 mm/min and the size of the sample was (5 × 5 × 7)mm.

* Corresponding author.
E-mail address: rksingh1978@yahoo.co.in (R.K. Singh).

0925-8388/$ – see front matter © 2010 Elsevier B.V. All rights reserved.
doi:10.1016/j.jallcom.2010.06.163

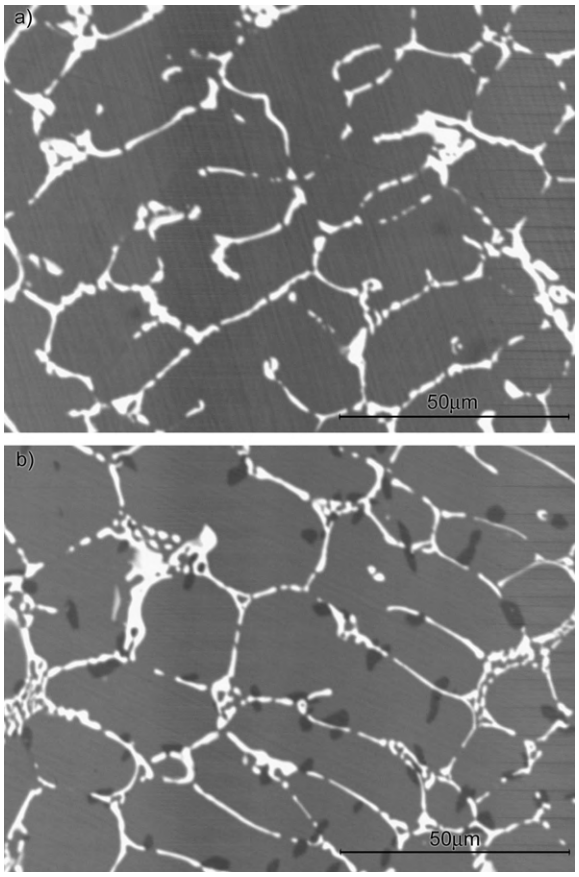

Fig. 1. Backscattered electron images of (a) FE5 and (b) FE10 alloys.

3. Results and discussions

3.1. Microstructure and phase analysis

Fig. 1a and b shows the typical back scattered electron (BSE) images of FE5 and FE10 alloys, respectively. It is evident that alloying addition markedly modifies the microstructure of the ternary NMG alloy. The NMG alloy exhibits a single-phase structure, whereas FE5 and FE10 alloys contain a second phase (white area) which is mainly distributed along the grain boundaries. A small volume fraction of an additional third phase (dark grey area) could also be identified in the BSE image of FE10 alloy. It can be seen in BSE image, that the second phase is mainly distributed along the grain boundaries while, the third phase in the FE10 alloy is precipitated both on the grain boundaries and inside the matrix phase, similar to the reported γ-phase distribution in Ni–Mn–Ga–Fe alloys [19]. The chemical composition of the constituent phases in NMG, FE5 and FE10 alloys analyzed by EPMA are summarized in Table 1. The chemical analysis clearly reveals that the intended amount of Fe goes into the matrix phase in both FE5 and FE10 alloys, whereas

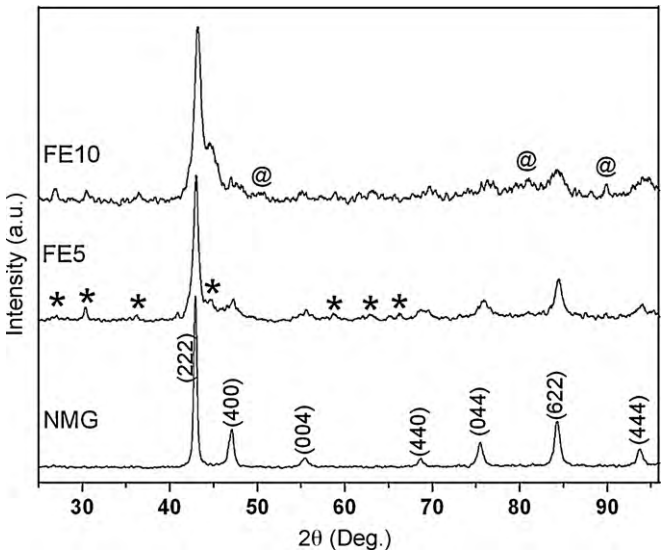

Fig. 2. X-ray diffraction patterns of NMG, FE5 and FE10 alloys recorded at room temperature.

rare-earths (Dy&Tb) shows negligible solubility in the matrix phase. The similar composition of the rare-earth rich phase in FE5 and FE10 alloys indicate that insolvable rare-earths segregates at the grain boundary and reacts with the matrix to form second phase. The additional third phase found only in FE10 alloy, which is essentially Fe-rich and free from rare-earths suggests that Fe has exceeded its maximum solid solubility in Ni–Mn–Ga matrix phase and forms precipitate with composition of the form $(Ni,Fe)_3(Mn,Ga)$.

X-ray powder diffraction (XRD) patterns of heat-treated alloys at room temperature are shown in Fig. 2. The XRD pattern of reference NMG alloy can be indexed to a single-phase tetragonal structure, corresponding to the typical non-modulated martensite observed in Ni–Mn–Ga alloys [4]. The XRD pattern for the FE5 can be indexed as mixture of two phases, with the main reflections corresponds to the tetragonal martensite phase of the Ni–Mn–Ga alloys and some minor reflections marked by (*) in Fig. 2. These extra peaks could correspond to the rare-earth rich phase present at the grain boundaries. For FE10 alloy, few more minor reflections marked as (@) in Fig. 2 could be identified, in addition to the reflections present in FE5 alloy which suggests that it contains three distinct phases, in accordance with the SEM results. However, the current XRD results are not enough to ascertain the structure of minor phases as overlapping of reflection does not permit indexing. Nonetheless, the XRD results clearly indicate that the matrix phase, which is the major phase in all the alloys, undergoes martensitic transformation.

3.2. Phase transformation and thermal analysis

In order to investigate the effect of alloying on the martensite transformation behavior, DSC measurements were carried out. The first order peaks corresponding to forward austenite to martensite

Table 1
Compositional analysis of the constituent phases in alloys studied.

Alloy	Constituent phase	Ni (at%)	Mn (at%)	Ga (at%)	Tb (at%)	Dy (at%)	Fe (at%)
NMG	Matrix	50.34	30.01	19.65	–	–	–
FE5	Matrix	48.55	28.85	17.47	–	–	5.13
	Second	54.59	11.22	17.87	4.16	7.73	4.43
FE10	Matrix	49.52	24.02	17.20	–	–	9.26
	Second	54.77	11.77	17.67	3.01	6.03	6.77
	Third	43.85	18.47	7.57	0.0	0.0	30.11

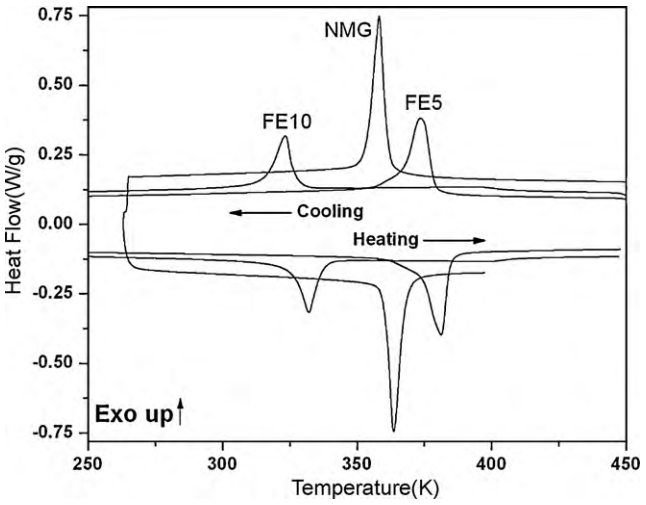

Fig. 3. DSC thermograms of NMG, FE5 and FE10 alloys.

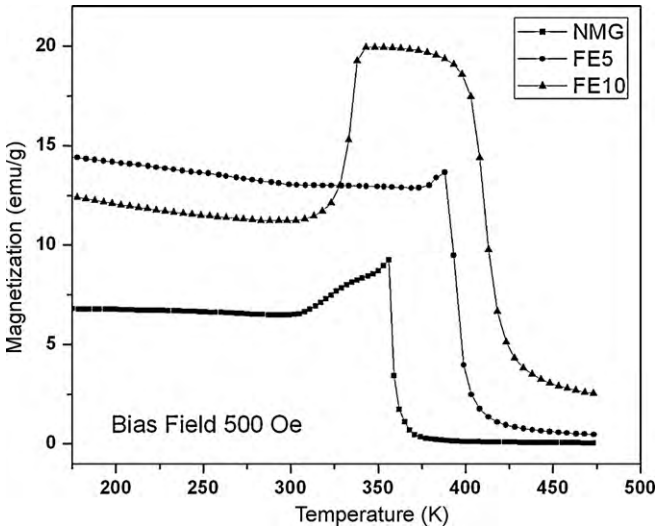

Fig. 4. Magnetization vs. temperature curves for the alloys studied.

transformation on cooling as well as reverse martensite to austenite transformation on heating can be clearly seen in DSC thermograms (Fig. 3). Table 2 list the critical transformation temperatures along with the enthalpy changes (ΔH) and hysteresis of martensite transformation (δT). The average value of heat exchanged during the forward and reverse martensite transformation was taken as ΔH, while the thermal hysteresis between the forward and the reverse transformation was calculated as $\delta T = A_f - M_s$. The martensite start temperature (M_s) exhibit non-monotonic dependence on Fe content of the alloys (Fig. 3). As compared to NMG alloy, M_s initially increases for FE5 alloy and then decreases for FE10 alloy. The variation in martensite transformation for FE5 and FE10 alloys could be related to the changes in the chemical composition of the matrix phase caused by the precipitation of rare-earth rich and Fe-rich phases. According to the EPMA results (Table 1), the rare-earth rich phase contains small amount of Mn, which causes significant enrichment of Mn in the matrix phase. This is in good agreement with the reported effect of rare-earth addition on the matrix composition in Ni–Mn–Ga ternary alloys [14,17]. However, with increase in Fe substitution for Mn (FE10 alloy), the Fe content in matrix phase is increased and, as a result, Fe-rich phase precipitate out and the martensite transformation temperature is decreased. From Table 2 it can be seen that the obtained ΔH values decreases with increase in Fe content of the matrix phase. This can be attributed to the decrease in the volume fraction of matrix phase that undergoes martensite transformation. Comparing the δT values in Table 2, it can be clearly seen that there is only a minor change in the hysteresis of transformation of the FE5 and FE10 alloys, signifying thermoelastic behavior of the martensite transformation. This clearly implies the role of precipitates in strengthening the austenite and martensite phase, such that, it hampers the process of generation of plastic strain during the phase transformation [20].

3.3. Magnetic properties

The Curie temperature for the alloys was determined by measuring magnetization as a function of temperature on heating (thermomagnetic curves) at a bias field of 500 Oe (Fig. 4). The high temperature inflection point in the curves were estimated as T_C and are listed in Table 2. From Fig. 4, it can be clearly seen that the T_C of NMG alloy is significantly enhanced by alloying. The T_C of NMG alloy is merged with the structural transformation temperatures (Table 2), whereas in FE5 and FE10 alloys the magnetic transition occurs in the austenite phase. This rise in T_C can be attributed to the increase in the Fe content of the matrix phase as rare-earths show negligible solid solubility in the matrix phase. The non-zero magnetization values beyond T_C in thermomagnetic curve of FE10 alloy (Fig. 4) indicates that the Fe-rich precipitate is ferromagnetic and has the T_C value higher than the matrix phase. The effect of such ferromagnetic phase on the room temperature magnetization curves of the alloys can be clearly seen in Fig. 5. The magnetization value of NMG alloy is initially lowered by the addition of Fe and rare-earths (FE5 alloy), however with increase in Fe content the ferromagnetic Fe-rich phase precipitates which enhances the net magnetization of the FE10 alloy. Magnetic measurements indicate that rare-earth rich phase do not contribute in improving the ferromagnetic function of the alloys as solubility of Fe and Mn in rare-earth rich phase is very low (Table 1).

3.4. Mechanical properties

In order to understand the effect of rare-earth and Fe addition on the mechanical properties of the NMG alloy, compressive tests were carried out at room temperature. Fig. 6 shows the compressive stress–strain curves of the alloys studied deformed to a total strain of 3%. The initial elastic deformation of the ternary NMG alloy terminates at a strain of about 1% and a stress of about 65 MPa, which corresponds to the elastic strain and martensite reorientation stress, respectively. The slow rise in stress value beyond 1% deformation is due to the reorientation of the martensite variants, although it does not exhibit a perfect stress plateau that could be due to the polycrystalline state of the sample. The defor-

Table 2
Transformation temperatures for the alloys studied.

Alloy	Martensite start temp. M_s (K)	Martensite finish temp. M_f (K)	Austenite start temp. A_s (K)	Austenite finish temp. A_f (K)	Enthalpy change ΔH (J/g)	Thermal hysteresis δT (K)	Curie temp. T_C (K)
NMG	362	353	359	370	9.281	8	363
FE5	379	360	365	385	8.751	6	408
FE10	329	314	326	338	5.186	9	429

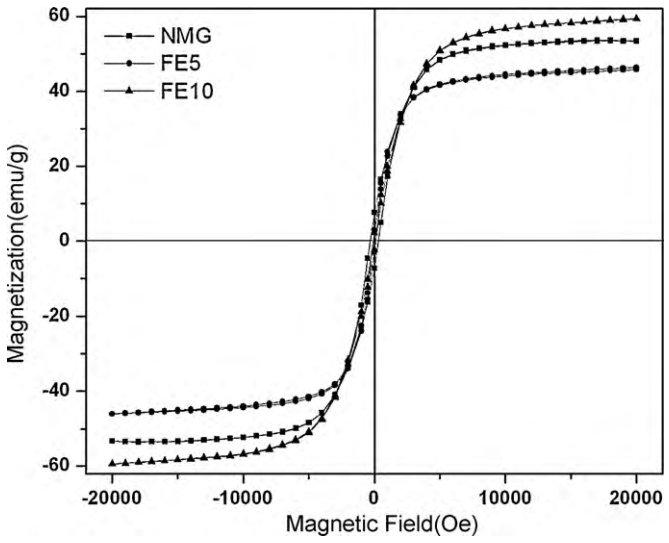

Fig. 5. Room temperature magnetization curves for NMG, FE5 and FE10 alloys.

mation behavior of FE5 and FE10 alloys are much complex. The stress plateau corresponding to reorientation of martensite variants disappears completely indicating that deformation in FE5 and FE10 alloys is dominated by dislocation movement. This change in deformation behavior could be due to the decrease in volume fraction of the martensite phase and precipitation of relatively ductile phases at grain boundaries in FE5 and FE10 alloys. Moreover, for same compressive stress value, FE5 and FE10 alloys exhibit larger strain values as compared to NMG alloy signifying that compressive ductility is enhanced by the formation of grain boundary phases. However, for FE10 alloy the Fe-rich phase is distributed inside the matrix as well which in turn has the negative effect on the compressive ductility.

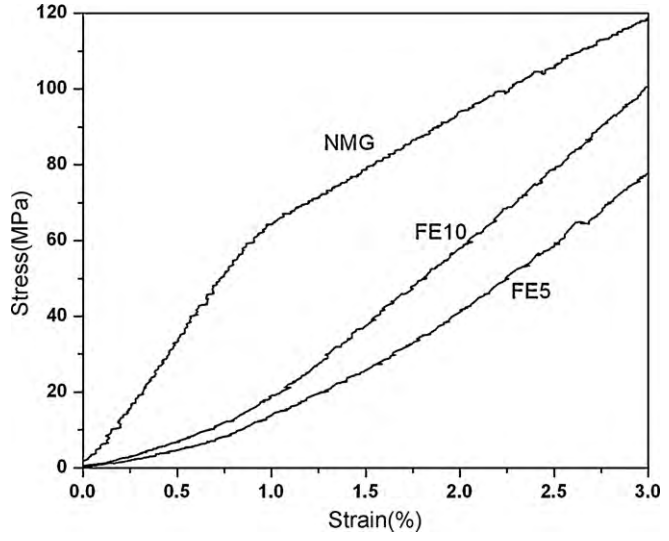

Fig. 6. The compressive stress–strain curves of NMG, FE5 and FE10 alloys.

4. Conclusion

The addition of rare-earths in Ni–Mn–Ga alloy was found to enhance the martensite transformation temperature and addition of Fe enhanced the Curie temperature of the $Ni_{50}Mn_{30}Ga_{20}$ alloy. The solubility limit of rare-earths in $L2_1$ matrix is very low and it causes formation of rare-earth rich phase at the grain boundary, while, Fe shows higher solid solubility in the $L2_1$ matrix. The compressive ductility was found to be enhanced by the precipitate distributed mainly at the grain boundaries. It was also found that the large hysteresis of martensite transformation observed in Ni–Mn–Ga–Fe alloys can be reduced by enhancing the strength of austenite and martensite phase.

Acknowledgements

The authors are grateful to Defense Research and Development Organization, Government of India for the financial support to carry out this work. The keen interest shown by Dr. V. Chandrasekaran and the Director, DMRL in this work is gratefully acknowledged.

References

[1] K. Ullako, J. Huang, C. Kantner, R.C. O'Handley, V.V. Kokorin, Appl. Phys. Lett. 69 (1996) 1966.
[2] V.A. Chernenko, S. Besseghini, Sens. Actuators A 142 (2008) 542.
[3] R.C. O'Hanely, S.J. Murray, M. Marioni, H. Nembach, S.M. Allen, J. Appl. Phys. 87 (2000) 4712.
[4] J. Pons, V.A. Chernenko, R. Santamarta, E. Cesari, Acta Mater. 48 (2000) 3027.
[5] I. Glavatskyy, N. Glavatska, O. Söderberg, S.-P. Hannula, U.-J. Hoffmann, Scripta Mater. 54 (2006) 1891.
[6] K. Koho, O. Söderberg, N. Lanska, Y. Ge, X. Liu, L. Straka, J. Vimpari, O. Heczko, V.K. Lindroos, Mater. Sci. Eng. A 378 (2004) 384.
[7] A.A. Cherechukin, V.V. Khovailo, et al., J. Magn. Magn. Mater. 258–259 (2003) 523.
[8] Z.H. Liu, M. Zhang, W.Q. Wang, W.H. Wang, J.L. Chen, G.H. Wu, et al., J. Appl. Phys. 92 (2002) 5006.
[9] V.V. Khovailo, V.A. Chernenko, A.A. Cherechukin, T. Takagi, T. Abe, J. Magn. Magn. Mater. 272–276 (2004) 2067.
[10] H.B. Wang, F. Chen, Z.Y. Gao, W. Cai, L.C. Zhao, Mater. Sci. Eng. A 438–440 (2006) 990.
[11] D. Soto, F.A. Hernandez, H. Flores, X. Moya, L. Manosa, A. Planes, S. Aksoy, M. Acet, T. Krenke, Phys. Rev. B 77 (2008) 184103.
[12] D. Kikuchi, T. Kanomata, Y. Yamaguchi, H. Nishihara, K. Koyama, K. Watanabe, J. Alloys Compd. 383 (2004) 184.
[13] F. Chen, H.B. Wang, Y.F. Zheng, W. Cai, L.C. Zhao, J. Mater. Sci. 40 (2005) 219.
[14] L. Gao, Z.Y. Gao, W. Cai, L.C. Zhao, Mater. Sci. Eng. A 438–440 (2006) 1077.
[15] L. Gao, J.H. Sui, W. Cai, J. Magn. Magn. Mater. 320 (2008) 63.
[16] W. Cai, L. Gao, A.L. Liu, J.H. Sui, Z.Y. Gao, Scripta Mater. 57 (2007) 659.
[17] R. Wroblewski, M. Leonowicz, Z. Zengqi, J. Liping, J. Magn. Magn. Mater. 316 (2007) e595.
[18] K. Tsuchiya, A. Tsutsumi, H. Ohtsuka, M. Umemoto, Mater. Sci. Eng. A 378 (2004) 370.
[19] Y. Xin, Y. Li, L. Chai, H. Xu, Scripta Mater. 57 (2007) 599.
[20] A.N. Vasil'ev, Buchel'nikov, T. Takagi, V.V. Khovailo, E.I. Estrin, Phys.-Usp. 46 (2003) 559.